

Studies on the Orientation and Polarized Photoluminescence of α -Naphthalene Acetate in the Layered Double Hydroxide Matrix

Wenyong Shi, Min Wei,* Jun Lu, David G. Evans, and Xue Duan

State Key Laboratory of Chemical Resource Engineering, Beijing University of Chemical Technology, Beijing 100029, P. R. China

Received: January 18, 2009; Revised Manuscript Received: May 23, 2009

This paper reports a novel method to tune the fluorescence properties of α -naphthalene acetate (α -NAA) in a two-dimensional matrix of layered double hydroxide (LDH) by changing the orientation of the chromophore. The α -NAA and 1-heptanesulfonic acid sodium (HES) with different molar ratios were co-intercalated in the galleries of Zn_2Al LDH by the anion exchange method. Thin films of α -NAA–HES/LDH ($x\%$, x stands for the molar percentage of α -NAA), which have a well c -orientation confirmed by the X-ray diffraction (XRD) and scanning electron microscopy (SEM), were obtained by the solvent evaporation method on Si substrates. On the basis of the results from XRD and fluorescence polarization, the orientation (Ψ angle) of the α -NAA molecule in the LDH matrix was calculated to be 59° ($x = 12.1\%$), 61° ($x = 15.1\%$), 64° ($x = 20.0\%$), 65° ($x = 23.3\%$), 68° ($x = 30.0\%$), and 71° ($x = 34.4\%$) with respect to the normal to the thin film, respectively. Furthermore, the fluorescence wavelength, emission intensity, and lifetime correlate with the orientation of α -NAA remarkably and can be finely controlled by varying the fluorophore content in a rigid and constrained environment of the host. The optimal luminous intensity and the longest fluorescence lifetime of α -NAA–HES/LDH ($x\%$) can be obtained with an x value ranging from 15 to 20%.

1. Introduction

Compounds of an organic chromophore and inorganic matrix offer a number of synergistic effects.¹ The inorganic host structure lends stabilization and protection, while the chromophore guest species provides optical functions such as color, fluorescence, or nonlinear optical properties. Layered inorganic materials with two-dimensional arrays in the nanoscale space domain are suitable systems with interesting applications in modified electrodes, chemical sensors, photochromic devices, and nonlinear optics.² In this sense, layered double hydroxides (LDHs) are important matrices which represent a large versatility in terms of their chemical composition and layer charge.³ LDHs can be represented by the general formula $[\text{M}_{1-x}\text{M}_x^{3+}(\text{OH})_2]^{x+}(\text{A}^{n-})_{x/n} \cdot m\text{H}_2\text{O}$, where M^{2+} and M^{3+} are metal cations and A^{n-} is an anion. The host structure consists of brucite-like layers of edge-sharing $\text{M}(\text{OH})_6$ octahedra, and the partial substitution of M^{3+} for M^{2+} induces positively charged host layers, balanced by the interlayer anions.⁴

The family of chromophore–LDH intercalation compounds provides an instructive example for optically functionalized inorganic–organic systems, providing materials with potential applications such as pigments or nonlinear optics or with other functionalities.^{5,6} Interestingly, it is feasible to orient the chromophore molecules by inclusion in the anisotropic inorganic host structure. Furthermore, the orientation of molecules intercalated in the LDH galleries has an important effect on the fluorescence properties of chromophores. Cooper and co-workers⁶ reported the intercalation of 4-nitrohippuric acid (NHA) between sheets of LDH, and the hybrid material exhibits frequency-doubling characteristics because of the ordered arrangement of molecular dipoles. Costantino et al.⁷ have reported that the fluorescence emission of methyl orange (MO) molecule

incorporated into Zn_2Al LDH can cover the whole visible wavelength range by changing the experimental conditions. Therefore, the key problem is how to effectively tune the molecular orientation of chromophores in the gallery of LDH to obtain controllable fluorescence performance. However, the lack of information about the accurate orientation of fluorophores intercalated in LDH prevents a more detailed and quantitative understanding of luminescent properties as well as the application of chromophore–LDH intercalation compounds in optical devices. It is therefore necessary to carry out investigations on the relationship between the luminescent properties of these materials and the orientation of fluorophores in the LDH matrix.

In our previous work,⁸ the fluorescence polarization method was applied to study the preferential orientation of α -NAA (α -naphthalene acetate) and β -NAA (β -naphthalene acetate) in the interlayer region of Zn_2Al LDH, respectively, and the results show that, for α -NAA and β -NAA, molecules are accommodated between sheets of Zn_2Al LDH as monomeric units with a tilt angle Ψ (defined as the angle between the transition moment of NAA with respect to the normal to the LDH layers) of 60° and 65° , respectively. The orientation investigation of α -NAA and β -NAA in the LDH matrix based on experimental techniques not only promotes profound insight for host–guest interactions but also provides fundamental information for the structural design and assembly of inorganic–organic intercalation compounds.

It was known that, besides the layer charge and hydration degree, the co-intercalated anion has a significant influence on the orientation and optical properties of the fluorophore in the LDH galleries.⁹ As a result, it can be expected that the orientation of the interlayer guest could be tuned by adjusting the kind and amount of the coexisting anions. In the present work, the cointercalation of α -NAA and 1-heptanesulfonic acid sodium (HES) with different molar ratios in the galleries of

* Corresponding author. Phone: +86-10-64412131. Fax: +86-10-64425385. E-mail: weimin@mail.buct.edu.cn.

Zn₂Al LDH was performed, to study the influences of HES on the orientation of α -NAA as well as on the fluorescence properties of the inorganic–organic intercalation compounds. HES was chosen as the dispersant because it possesses a similar length to α -NAA at the vertical direction. The coexisting HES plays an important role on the orientation and photoemission properties of α -NAA. First, it prevents the aggregation of α -NAA and adjusts the orientation of α -NAA through different molar ratios of α -NAA/HES. Second, it provides the α -NAA fluorophore with a homogeneous and nonpolar environment and thus enhances its luminescent performances. The α -NAA–HES/LDH samples with different molar ratios were prepared by the ion-exchange method, and then their thin films on Si substrates were obtained by the solvent evaporation method. It was found with the fluorescence polarization technique that the molecular anion orientation Ψ of α -NAA increases from 59° to 71° with the increase of its molar percentage (12.1%, 15.1%, 20.0%, 23.3%, 30.0%, and 34.4%). Furthermore, the fluorescence wavelength, emission intensity, and lifetime correlate with the orientation of α -NAA remarkably and can be finely controlled by varying the fluorophore content in a rigid and constrained environment of the host. Therefore, this work provides a novel strategy for accurately modulating the photoluminescent properties (wavelength, emission intensity, and lifetime) of chromophore–LDH materials by simply changing the relative loading of the chromophore and coexisting anion in the LDH matrix.

2. Experimental Section

2.1. Materials. Sodium α -NAA and HES (biochemistry grade) were purchased from Sigma-Aldrich Company. Analytical grade chemicals including Zn(NO₃)₂·6H₂O, Al(NO₃)₃·9H₂O, NaOH, etc., were purchased from the Beijing Chemical Co. Limited and used without further purification. The deionized and de-CO₂ water was used in all of these experimental processes.

2.2. Synthesis of the α -NAA and HES Co-intercalated Zn₂Al LDH. The Zn₂Al–NO₃ LDH precursor was synthesized by the hydrothermal method reported previously.¹⁰ The pH of the aqueous solution (200 mL) containing 0.08 mol Zn(NO₃)₂·6H₂O and 0.04 mol Al(NO₃)₃·9H₂O was adjusted to 8.5 with NH₃·H₂O, and it was aged in an autoclave at 140 °C for 10 h. The precipitate was centrifuged and washed thoroughly with water. Subsequently, the α -NAA and HES co-intercalated LDH compounds were prepared following the ion-exchange method. α -NAA (*a* mol) and HES (*b* mol) were dissolved in 150 mL of water/ethanol mixture solvent (1:1, v/v), in which *a* + *b* = 0.004 mol and *a*:*b* = 100:0, 100:14, 100:18, 100:24, 100:25, 100:55, 100:62, and 0:100, respectively. Freshly prepared Zn₂Al–NO₃ LDH (0.5 g) was dispersed in the solution thoroughly. The suspension was adjusted to pH = 8.0 with a NaOH (0.2 mol/L) solution and held at room temperature under N₂ atmosphere for 48 h. The product α -NAA–HES/LDH (*x*%, *x* = *a*/(*a* + *b*)) was washed extensively with water.

2.3. Fabrication of α -NAA–HES/LDH (*x*%) Thin Films. Thin films of α -NAA–HES/LDH (*x*%) were fabricated by the solvent evaporation method. Substrates of Si wafer were first cleaned by immersing in a bath of H₂SO₄/H₂O₂ (3:1, v/v) in an ultrasonic bath for 30 min. Pasty α -NAA–HES/LDH (*x*%) (0.05 g) was suspended in 20 mL of water under N₂ atmosphere in an ultrasonic bath (99 W, 28 kHz) at room temperature for 5 min. Then, the resulting α -NAA–HES/LDH (*x*%) suspension was dropped on Si substrates and dried in vacuum at ambient temperature for 5 h.

2.4. Techniques of Characterization. The powder X-ray diffraction (XRD) measurements were performed on a Rigaku XRD-6000 diffractometer, using Cu K α radiation (λ = 0.15418 nm) at 40 kV, 30 mA, with a scanning rate of 5°/min, and a 2θ angle ranging from 3° to 65°. Scanning electron microscopy (SEM) images were obtained using a Hitachi S-4700 scanning electron microscope operating at 20 kV. The ultraviolet–visible (UV–vis) spectra were collected in a Shimadzu U-3000 spectrophotometer. Fluorescence emission spectra were recorded on a RF-5301PC fluorophotometer (1.5 nm resolution) in the range of 290–500 nm with the excitation wavelength of 280 nm and slit widths of 3 nm. Elemental analysis samples were prepared by dissolving 30 mg of solid sample with a few drops of concentrated HNO₃ and diluting to 50 mL with water. Zn, Al, and S elemental analyses were performed by atomic emission spectroscopy with a Shimadzu ICPS-7500 instrument. C, H, and N content was determined using an Elementar vario elemental analysis instrument. The water content of the sample was obtained by thermogravimetry.

Fluorescent Decay. The curves were recorded by means of the time-correlated single-photon counting technique employing a LifeSpec-red lifetime spectrometer (Edinburgh Instruments Ltd., U.K.), which is equipped with an emission double monochromator and a time resolution of 25 ps after deconvolution of the excitation pulse. From the recorded fluorescence decay curves, two different analyses can be performed for the recorded data based on two experimental setups.

i. Fluorescence Lifetime Analysis. For a fixed emission wavelength, the fluorescence decay curve was collected. The lifetime of the samples was obtained from the recorded decay curves after deconvolution of the instrument response function (IRF) was carried out by an iterative method of nonlinear least-squares based on the Marquardt algorithm. The fluorescence decay curves were analyzed at an emission wavelength of 337 nm for α -NAA–HES/LDH (*x*%).

ii. Time-Resolved Emission Spectra (TRES). Fluorescence decay curves were recorded as a function of the emission wavelength in the range of 320–440 nm for α -NAA–HES/LDH (*x*%) (wavelength increment of 1 nm) for a fixed recording time (200 s per wavelength). The emission spectra at different times after excitation were obtained by averaging the integrated fluorescence intensity for fixed time windows of 3 ns at every wavelength in the 28, 34, 35, 29, 27, and 26 ns time interval for α -NAA–HES/LDH (*x*%) after the 280 nm excitation pulse (ps).

Fluorescence Polarization. The spectra were recorded on a Quanta Master-Spectrofluorometers (model QM-4/2005), equipped with automated polarizers in both the excitation and the emission beams. The three-dimensional perspective for the experimental setup has been provided in the Supporting Information (Figure S1). The fluorescence spectra of the thin film were registered after excitation at 280 nm for α -NAA–HES/LDH (*x*%), where the fluorescence emission was collected along the Z'-axis at 90° with respect to the excitation beam in the Z-axis. The fluorescence polarization spectra were scanned in the range of 300–400 nm every 1 nm, with an integration time of 2 s and excitation and emission slits of 8 nm.

The orientation of the thin film with respect to the excitation beam was changed by rotating the solid-sample holder around its vertical y-axis. Indeed, the angle between the normal to the thin film and the excitation axis (defined as the δ angle in Figure S1) was scanned from 0° to 60°. The instrumental response to the linearly polarized light has been corrected by recording the fluorescence signal of an isotropic system under identical

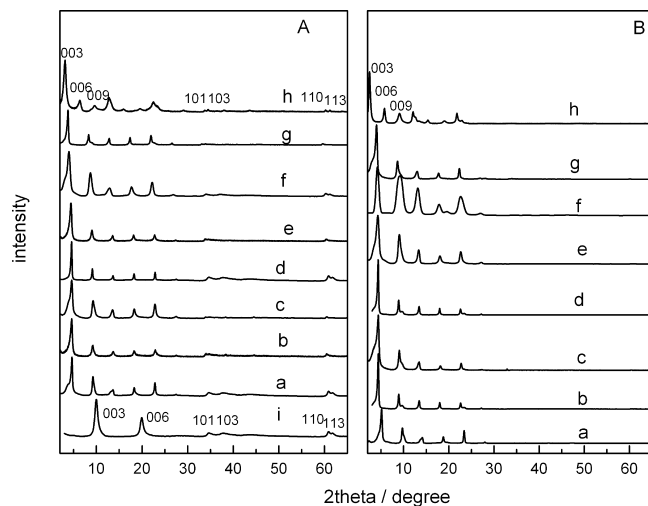


Figure 1. (A) XRD patterns for powder samples: (a–h) α -NAA–HES/LDH ($x\%$), (i) $\text{Zn}_2\text{Al-NO}_3$ LDH. (B) XRD patterns for thin film samples: (a–h) α -NAA–HES/LDH ($x\%$). (a–h) $x = 0, 12.1\%, 15.1\%, 20.0\%, 23.3\%, 30.0\%, 34.4\%$, and 100% , respectively.

experimental conditions. In the present work, the same sample was used as the isotropic system.

3. Results and Discussion

3.1. Macroscopic Orientation of α -NAA–HES/LDH ($x\%$). The XRD patterns of $\text{Zn}_2\text{Al-NO}_3$ LDH and α -NAA–HES/LDH ($x\%$) are shown in Figure 1. All of the patterns of these samples can be indexed to a hexagonal lattice. The interlayer spacing can be calculated from averaging the positions of the three harmonics: $c = (1/3)(d_{003} + 2d_{006} + 3d_{009})$. The (003) reflection of $\text{Zn}_2\text{Al-NO}_3$ LDH powder at $2\theta = 9.9^\circ$ (Figure 1A, curve i) indicates an interlayer distance of 0.88 nm. The basal spacing of α -NAA–HES/LDH ($x\%$) (Figure 1A, curve a–h) increases from 1.68 nm ($x = 0$) to 2.81 nm ($x = 100\%$), indicating that α -NAA and HES were co-intercalated into the galleries of LDH. The different interlayer distance of pristine HES/LDH (1.68 nm) and α -NAA/LDH (2.81 nm) for similar molecular anion length (1.01 nm for α -NAA and 1.10 nm for HES, calculated by Chemwin 6.0) results from different arrangement and the orientation of the guest in the interlayer region of LDH. Moreover, the variation of the basal spacing can be attributed to the different arrangements of interlayer guest molecules resulted from different ratios of α -NAA/HES. It can be seen that α -NAA–HES/LDH ($x\%$) (Figure 1B) has only one series of (00 l) reflections. The half-peak width (fwhm) of the (003) reflection (0.31° – 0.54°) for all of the α -NAA–HES/LDH ($x\%$) samples (Figure S2B) is less than that of the precursor ZnAl-NO_3 –LDH (0.75°) (Figure S2A); that is, no broadening of the (003) reflection of LDH occurs after cointercalation of α -NAA and HES. Moreover, a good linear relationship between d_{003} and x in the x range of 12.1% – 34.4% (Figure S3) was observed with less error ($\leq 3\%$). Both indicate that α -NAA and HES disperse uniformly in the galleries of LDH, forming a homogeneous phase. The Fourier transform infrared (FT-IR) spectra further confirmed the cointercalation of the two anions (see Figure S4 in the Supporting Information). The chemical compositions of resulting products corresponding to different nominal concentrations are given in Table 1. It can be seen that the experimental ratio of α -NAA to HES in the samples of α -NAA–HES/LDH ($x\%$) is close to the nominal ratio as expected. Moreover, the XRD profiles of α -NAA–HES/LDH ($x\%$) film samples (Figure 1B) only reveal (00 l) reflections,

indicating a highly ordered stacking of the LDH layers in the c -direction normal to the supporting surface. Similarly to the α -NAA–HES/LDH ($x\%$) powder samples, the (003) reflection of the thin film also progressively shifts to lower 2θ values by increasing the α -NAA content, implying a reorientation of α -NAA anion. A larger packing of the chromophore molecules in the interlayer space probably leads to a more perpendicular disposition of the molecules and improves the stacking of the LDH layers.¹¹

SEM images of the α -NAA–HES/LDH ($x\%$) are displayed in Figure 2. The powder samples of α -NAA–HES/LDH ($x\%$) afford a rough surface, and high magnification SEM images (Figure 2a₁–f₁) reveal that they are composed of randomly oriented LDH particles with irregular morphology. In contrast, the thin films of α -NAA–HES/LDH ($x\%$) exhibit a surprisingly smooth and continuous surface in the top view (Figure 2a₂–f₂). High magnification SEM images of the thin films (Figure 2a₃–f₃) demonstrate that the individual α -NAA–HES/LDH ($x\%$) platelets are densely packed on the substrate plane. The SEM images confirm that the thin films are fabricated with a well c -orientation of α -NAA–HES/LDH ($x\%$) platelets, consistent with their XRD results in Figure 1.

3.2. Study on the Orientation of α -NAA Intercalated in LDH Matrix.

3.2.1. Orientation of Transition Dipole Moment for α -NAA. For π – π^* transitions of aromatic hydrocarbons, the absorption transition moments are in the plane of the molecule, whose direction with respect to the molecular axis depends on the electronic state attained on excitation. In the case of naphthalene and anthracene, the transition moment is oriented along the short axis for the $S_0 \rightarrow S_1$ transition and along the long axis for the $S_0 \rightarrow S_2$ transition.¹² Indeed, it has been reported that the main absorption band and the fluorescence emission of NAA involve $S_0 \rightarrow S_1$ singlet states.¹³ Therefore, the transition is oriented along the short molecular axis, as quantum mechanic calculations suggested, and this is illustrated in the structure of α -NAA (Scheme 1).

3.2.2. Determination of Orientation for α -NAA Intercalated in LDH by Polarized Fluorescence. Polarized fluorescence,¹⁴ resulted from the ordered arrangement of chromophores, can be employed as a structural probe for the orientation of the interlayer guest in the LDH matrix, since it provides useful information on molecular mobility, size, shape, and flexibility, fluidity of a medium, and order parameters.¹³ This method is based on the different responses of the fluorescence spectra of the sample to the horizontal (I_{VH}) and vertical directions (I_{VV}) of the emission polarizer (keeping the excitation polarizer constant in the vertical direction) for different orientations of the sample with respect to the excitation beam (the normal to the film was twisted at a δ angle). A linear relationship between the fluorescence dichroic ratio (D_{HV} defined as the ratio of H and V polarized emission spectra, $D_{\text{HV}} \equiv I_{\text{VH}}/I_{\text{VV}}$) and the twist angle δ was established by means of

$$D_{\text{HV}} = \frac{I_{\text{VH}}}{I_{\text{VV}}} = 2 \cot^2 \psi + (1 - 2 \cot^2 \psi) \cos^2(90 + \delta) \quad (1)$$

From the corresponding slope and/or intercept, the orientation of the chromophore (Ψ angle, defined as the angle between the transition moment of the chromophore and the normal to the host layer) can be evaluated. In our previous work, the validity of eq 1 was checked for α -NAA LDH and β -NAA LDH film, and a preferential orientation of α -NAA and β -NAA of 60°

TABLE 1: Chemical Compositions of α -NAA–HES/LDH ($x\%$) with Different α -NAA Content

nominal content x (%)	chemical composition	Zn/Al ration	experimental content x (%)
0	$[\text{Zn}_{0.68}\text{Al}_{0.32}(\text{OH})_2](\text{HES})_{0.32} \cdot 1.59\text{H}_2\text{O}$	2.13	0
12.5	$[\text{Zn}_{0.67}\text{Al}_{0.33}(\text{OH})_2](\alpha\text{-NAA})_{0.04}(\text{HES})_{0.29} \cdot 0.49\text{H}_2\text{O}$	2.03	12.1
15.6	$[\text{Zn}_{0.67}\text{Al}_{0.33}(\text{OH})_2](\alpha\text{-NAA})_{0.05}(\text{HES})_{0.28} \cdot 1.06\text{H}_2\text{O}$	2.03	15.1
18.7	$[\text{Zn}_{0.65}\text{Al}_{0.35}(\text{OH})_2](\alpha\text{-NAA})_{0.07}(\text{HES})_{0.28} \cdot 0.88\text{H}_2\text{O}$	1.86	20.0
20.5	$[\text{Zn}_{0.69}\text{Al}_{0.31}(\text{OH})_2](\alpha\text{-NAA})_{0.08}(\text{HES})_{0.23} \cdot 0.33\text{H}_2\text{O}$	2.22	23.3
35.5	$[\text{Zn}_{0.67}\text{Al}_{0.33}(\text{OH})_2](\alpha\text{-NAA})_{0.10}(\text{HES})_{0.23} \cdot 0.37\text{H}_2\text{O}$	2.03	30.0
38.2	$[\text{Zn}_{0.68}\text{Al}_{0.32}(\text{OH})_2](\alpha\text{-NAA})_{0.11}(\text{HES})_{0.21} \cdot 0.92\text{H}_2\text{O}$	2.13	34.3
100	$[\text{Zn}_{0.66}\text{Al}_{0.34}(\text{OH})_2](\alpha\text{-NAA})_{0.34} \cdot 1.20\text{H}_2\text{O}$	1.94	100

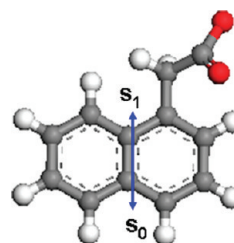
and 65° with respect to the layer LDH normal was obtained, respectively.⁸

Equation 1 was derived in the absence of any depolarization phenomena affecting the recorded anisotropy behavior in the fluorescence.¹⁵ In this sense, the following aspects are required for eq 1 to be applicable: parallel orientation between the absorption and the fluorescence transition dipole moments of the fluorophore, absence of rotational motions of the adsorbed fluorophores during their fluorescence lifetime, and absence of any excitation energy migration and/or transfer processes or any reabsorption/reemission phenomena, which could induce a change in the orientation of the transition moment from the excited state directly populated in the excitation process to the fluorescence excited state of the recorded emission intensity.

For the α -NAA–HES/LDH ($x\%$) films, the main absorption band and the fluorescence emission of α -NAA involve common S_0 and S_1 singlet states. First, the reorientation of the adsorbed α -NAA molecules during their fluorescence can be ruled out, as the time-correlated fluorescence decay curves of α -NAA–HES/LDH ($x\%$) films do not exhibit any dependence on the orientation of the emission polarizer after excitation with vertically polarized pulses (see Section 3.3.3). Second, the absence of time-dependent fluorescence anisotropy reveals a static adsorption of the dye molecules in the time scale of the fluorescence lifetime (around 28 ns) (see Section 3.3.3). Therefore, eq 1 can be used to evaluate the orientation of α -NAA in the α -NAA–HES/LDH ($x\%$) films.

Figure 3A–F displays the fluorescence spectra of α -NAA–HES/LDH ($x = 12.1\%, 15.1\%, 20\%, 23.3\%, 30\%,$ and 34.4% ,

SCHEME 1: Structure and Orientation of the Transition Dipole Moment for α -NAA



respectively) thin films recorded with the emission polarizer in the V (I_{VV}) and H (I_{VH}) directions for different twist δ angles. These fluorescence spectra were corrected for the instrumental response to the emission V and V polarizer, taking into account the evolution of the fluorescence band of an isotropic system with the twist angle δ recorded under identical conditions. The fluorescence intensity for the emission V polarizer increases by increasing the twist angle δ from 0° up to 60° (Figure 3A₁–F₁). These evolutions are also observed for the H polarized emission light (Figure 3A₂–F₂). These evolutions corroborate the fluorescence anisotropy behavior of α -NAA–HES/LDH ($x\%$) thin films, which are assigned to the preferential orientation of the α -NAA molecule in LDH galleries. Moreover, the change in the shape of fluorescence spectra can be observed upon changing the twist angle δ or the direction of emission polarizer, which may root in the scattered light from different directions (both horizontal and vertical).¹⁶

The fluorescence anisotropy is analyzed by the dichroic parameter ($D_{H,V}$). Because of the intrinsic instrumental

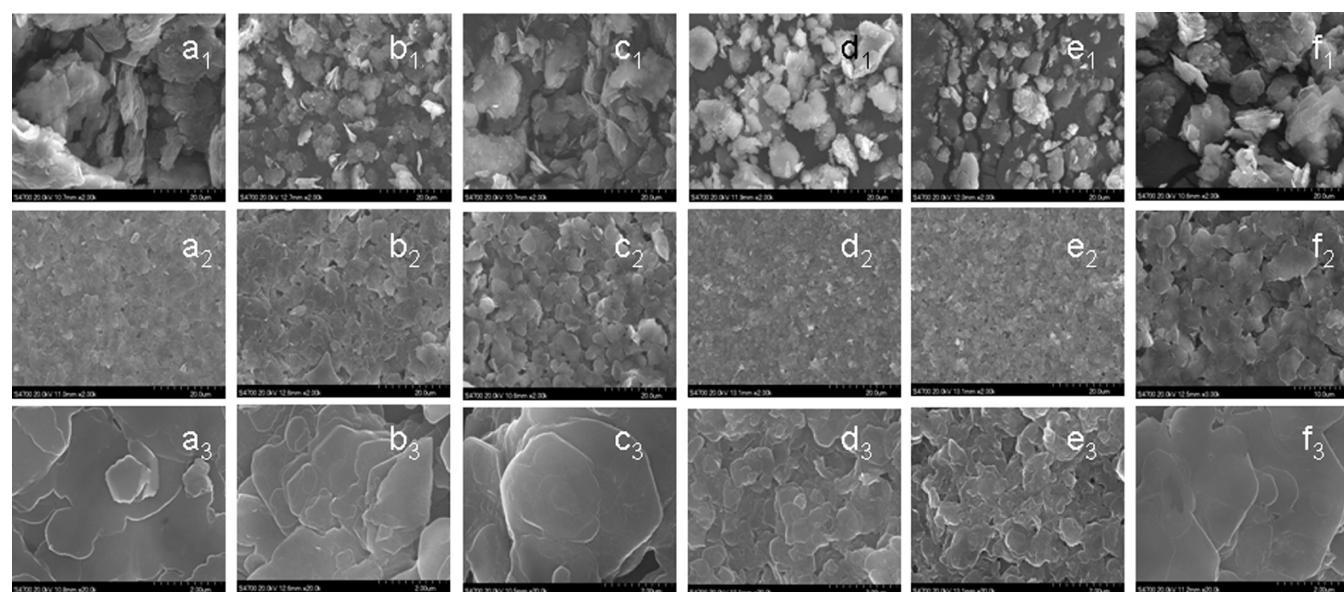


Figure 2. SEM images for α -NAA–HES/LDH ($x\%$) powder samples from a_1 to f_1 ; thin film samples at low magnification from a_2 to f_2 and high magnification from a_3 to f_3 ($x = 12.1\%, 15.1\%, 20.0\%, 23.3\%, 30.0\%,$ and 34.4% , respectively).

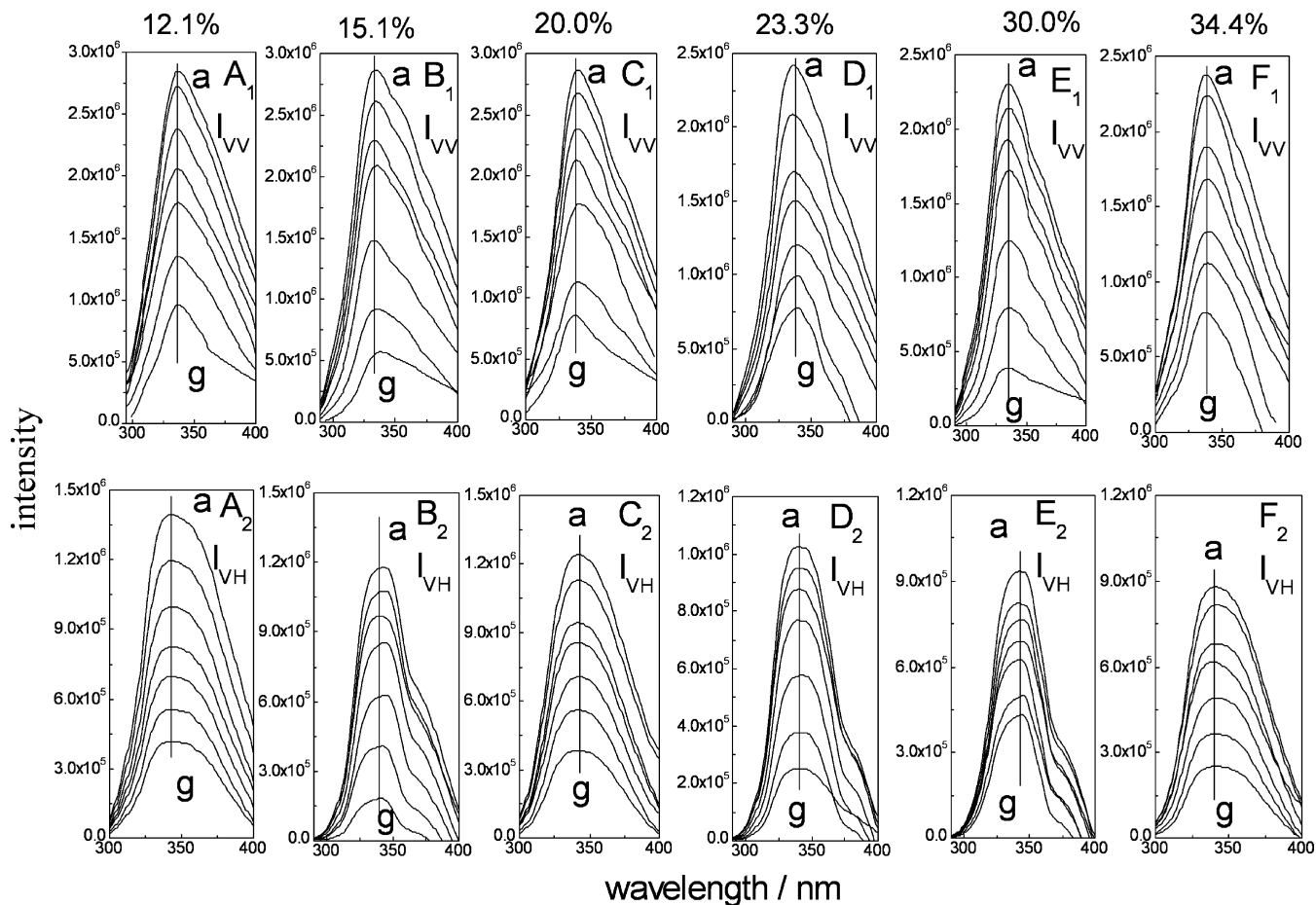


Figure 3. Evolution of the V (A_1 – F_1 ; $x\%$) and H (A_2 – F_2 ; $x\%$) ($x = 12.1\%$, 15.1% , 20.0% , 23.3% , 30.0% , and 34.4% , respectively) polarized fluorescence spectra of the α -NAA–HES/LDH ($x\%$) thin films with the following twist angles δ of the sample: (a) 60° , (b) 50° , (c) 40° , (d) 30° , (e) 20° , (f) 10° , and (g) 0° . Spectra were recorded after excitation with vertical polarized light.

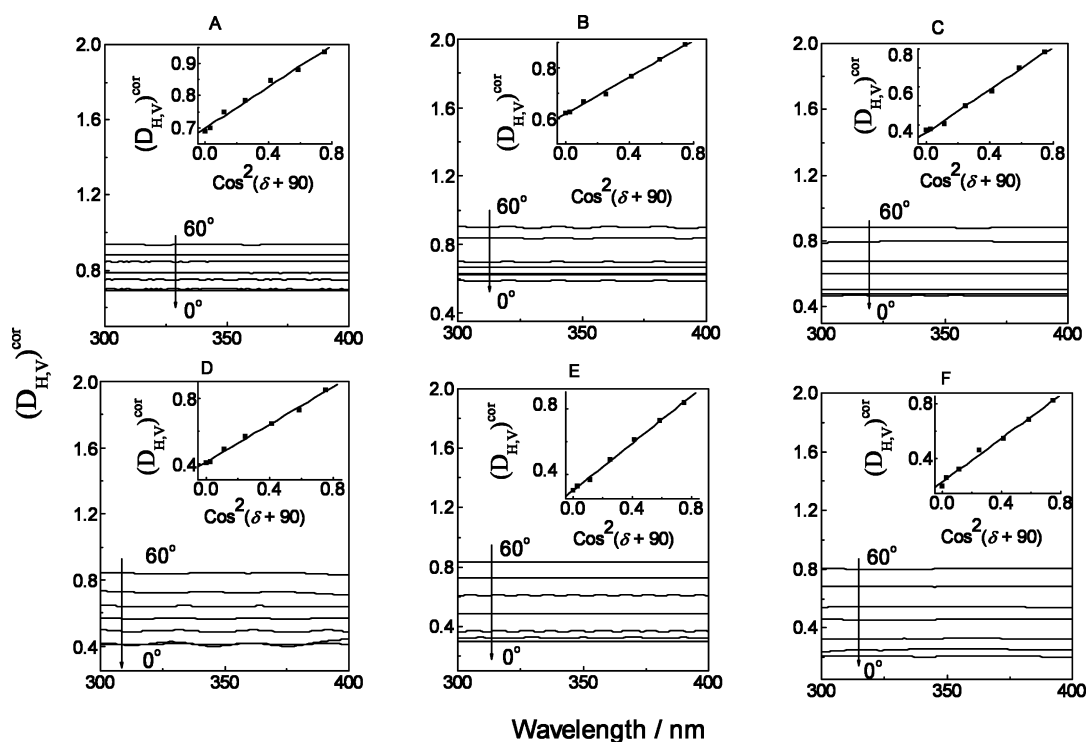


Figure 4. Evolution of the fluorescence dichroic ratio of the α -NAA–HES/LDH ($x\%$) thin films with the emission wavelength for different twisting δ angles of the sample (see Figure 3 caption): (A–F) $x = 12.1\%$, 15.1% , 20.0% , 23.3% , 30.0% , and 34.4% , respectively. The linear relationship between the dichroic ratio and $\cos^2(\delta + 90)$ at 350 nm is included in the inset graph.

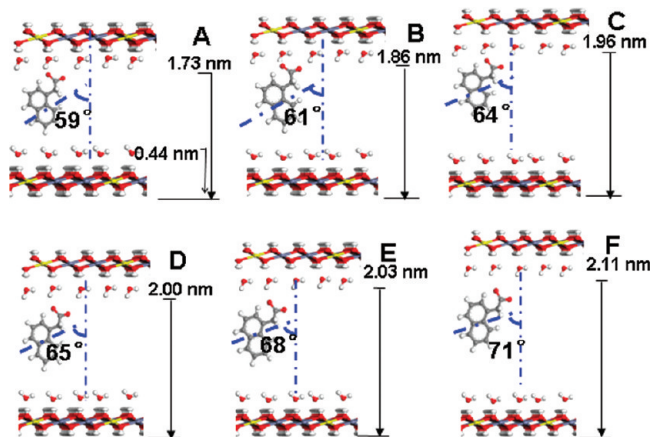


Figure 5. Schematic representation for the orientation of α-NAA in the α-NAA-HES/LDH (x%) materials: (A) 12.1%, (B) 15.1%, (C) 20.0%, (D) 23.3%, (E) 30.0%, and (F) 34.4% (Zn blue, C gray, H white, Al yellow, O red).

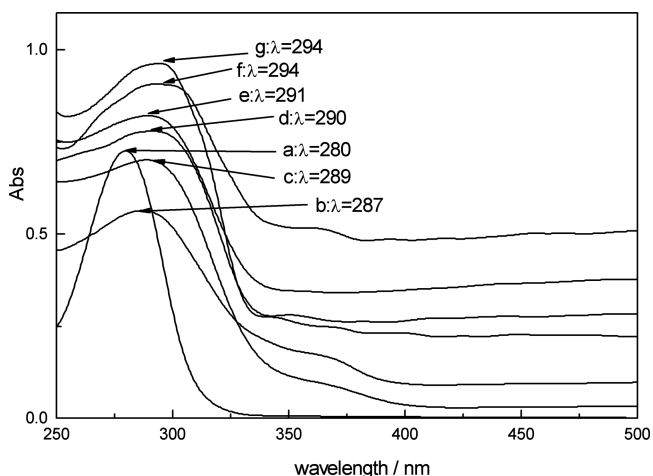


Figure 6. UV-vis absorption spectra of (a) pristine α-NAA in solution and the α-NAA-HES/LDH (x%) samples for (b) x = 12.1%, (c) x = 15.1%, (d) x = 20.0%, (e) x = 23.3%, (f) x = 30.0%, and (g) x = 34.4%.

response to the plane of the polarized light, D_{HV} has to be corrected for the response of the detection channel to the H and V polarization, by means of $(D_{HV})^{cor} = I_{VH}/I_{VV} \times G$ (G is the instrumental G factor determined by the recorded fluorescence anisotropy of an isotropic system, $G \equiv (I_{HV}/I_{HH})^{iso}$). In this work, the same sample was used as the isotropy system (see the Experimental Section for further details). The evolution of the fluorescence dichroic ratio with the emission wavelength of α-NAA-HES/LDH (x%) thin films for different twist δ angles is shown in Figure 4A-F. For a given δ angle, the $(D_{HV})^{cor}$ value is practically independent of the emission wavelength, confirming the presence of only one type of α-NAA species for these experimental samples. The augmentation of the $(D_{HV})^{cor}$ value at shorter wavelengths for small δ angles can be attributed to an incomplete correction of the scattering of the excitation light observed in thin film samples (not shown).

For a given emission wavelength, the dichroic ratio of α-NAA-HES/LDH (x%) thin film samples linearly correlates with the $\cos^2(90 + \delta)$ value, as shown in the inset of Figure 4A-F at 350 nm. According to eq 1, the orientation Ψ angle between the transition moment of the fluorescent species and

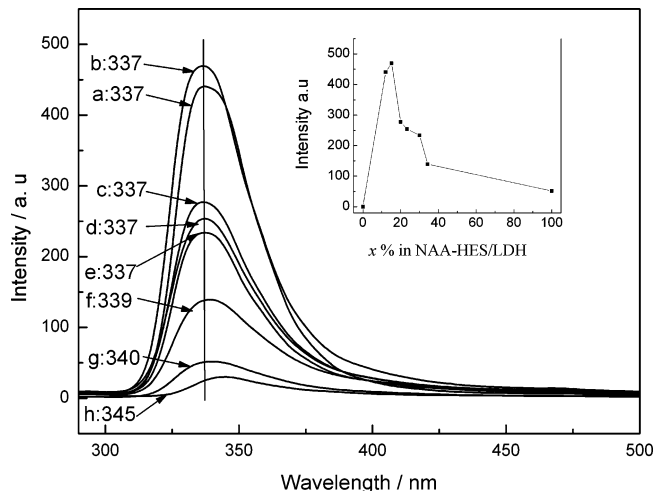


Figure 7. Photoemission spectra of α-NAA-HES/LDH (x%) for (a) x = 12.1%, (b) x = 15.1%, (c) x = 20.0%, (d) x = 23.3%, (e) x = 30.0%, (f) x = 34.4%, (g) 100%, and (h) pristine α-NAA solid powder with the excitation wavelength of 280 nm. The inset plot shows the fluorescence intensity varying with the increase of α-NAA content in the α-NAA-HES/LDH (x%).

the normal to the LDH layer can be evaluated from the slope and/or intercept of this linear relationship:

$$(D_{HV})^{cor} = \frac{I_{VH}}{I_{VV}} \times G = 2 \cot^2 \psi + (1 - 2 \cot^2 \psi) \cos^2(90 + \delta) \quad (2)$$

The good linear relationship observed in this representation, with a correlation coefficient $r > 0.99$, indicates the validity of the above assumptions related with the absence of any depolarization phenomena during the excited state lifetime of the α-NAA-HES/LDH (x%) thin film samples as well as of the powerful application of the fluorescence polarization method to evaluate the orientation of the α-NAA molecule in the LDH matrix. Similar plots were observed for other emission wavelengths. From the slope and intercept of the $(D_{HV})^{cor}$ versus $\cos^2(90 + \delta)$ linear relationship shown in the inset of Figure 4A-F, the orientation Ψ angles of α-NAA molecule were calculated to be 59° (x = 12.1%), 61° (x = 15.1%), 64° (x = 20.0%), 65° (x = 23.3%), 68° (x = 30.0%), and 71° (x = 34.4%), respectively. Therefore, the results above confirm that the orientation of the α-NAA chromophore in the LDH matrix can be tuned by adjusting the relative content of α-NAA and the dispersant.

3.2.3. Molecular Models of α-NAA Intercalated LDH. On the basis of the experimental conditions with a solution pH of 8.0, α-NAA exists mainly as the monovalent anion ($pK_a = 4-5$) during the ion-exchange process. The d_{003} spacing of α-NAA-HES/LDH (x%) ranges in 1.73–2.11 nm obtained from XRD results. If the thickness of the LDH layer (0.44 nm)⁷ is subtracted from the basal spacing, the values of gallery height are calculated to be 1.29, 1.44, 1.52, 1.57, 1.59, and 1.67 nm, respectively. These values are larger than the length of either the α-NAA or HES anion (1.01 nm for α-NAA and 1.10 nm for HES, calculated by Chemwin 6.0). Comparison of the length of the α-NAA and HES anions with the gallery height suggests that α-NAA and HES are accommodated in the interlayer region as a monolayer or interdigitated bilayer, in which the carboxyl and sulfonic group of individual anion interacts electrostatically with Al³⁺ cation in the LDH layers. FT-IR spectroscopy confirms

TABLE 2: Fluorescence Decay Data of α -NAA in Solution and the α -NAA–HES/LDH ($x\%$) Samples^a

x (%)	n	τ_i (ns)	A_i (%)	$\langle\tau\rangle$ (ns)	χ^2/dof	r^2
12.1%	1	28.6	100	28.9	0.00007	0.9984
	2	20.7	18.8		0.0001	0.9854
		30.8	81.2			
15.1%	1	34.7	100	33.2	0.00004	0.9985
	2	23.4	15.5		0.0002	0.9954
		35.0	84.5			
20.0%	1	35.2	100	35.0	0.00002	0.9996
	2	26.7	8.8		0.0002	0.9956
		35.8	91.2			
23.3%	1	29.4	100	30.2	0.00002	0.9984
	2	23.3	10.4		0.0001	0.9942
		31.0	89.6			
30.0%	1	27.9	100	27.4	0.00006	0.9988
	2	26.4	44.7		0.0002	0.9715
		28.2	55.3			
34.4%	1	26.0	100	26.5	0.00007	0.9987
	2	19.8	34.4		0.0002	0.9623
		30.0	65.6			
solution, 10^{-5} mol/L	1	28.5	100		0.00002	0.9996

^a τ is the fluorescence lifetime, and $\langle\tau\rangle$ is the intensity average lifetime. The goodness of fit is indicated by the value of χ^2/dof and r^2 .

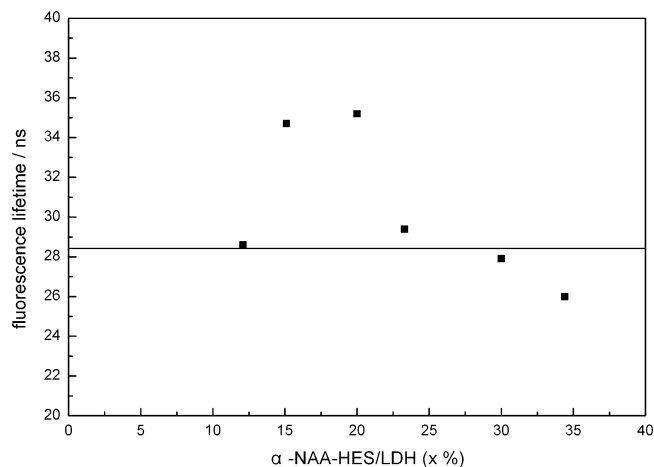


Figure 8. Fluorescence lifetime of α -NAA–HES/LDH ($x\%$) as a function of $x\%$. The horizontal line represents the fluorescence lifetime of α -NAA in solution (10^{-5} mol/L).

the formation of the hydrogen bonding system in the α -NAA–HES/LDH ($x\%$) materials. The FT-IR spectra of $\text{Zn}_2\text{Al–NO}_3$ LDH, α -NAA, HES intercalated LDH, and α -NAA–HES/LDH ($x\%$) are shown in Figure S4. Compared with the pristine α -NAA (Figure S4b), the symmetric and asymmetric carboxylate stretching bands of the intercalated α -NAA (Figure S4d–i) shift to lower frequency (from 1407 to ~ 1380 cm^{-1} and from 1693 to ~ 1560 cm^{-1}), indicating that the carboxylate group in α -NAA is involved in the formation of hydrogen bonding. Moreover, compared with the $\text{Zn}_2\text{Al–NO}_3$ LDH precursor, the O–H stretching absorption band of α -NAA–HES/LDH ($x\%$) shifts to a lower frequency, that is, from 3519 cm^{-1} for the former (Figure S4a) to ~ 3470 cm^{-1} for the latter (Figure S4d–i). This indicates that the hydroxyl group of LDH host layers also participates in the formation of hydrogen bonding. On the basis of the above discussion, the representational molecular models for the orientation of α -NAA in the α -NAA–HES/LDH ($x\%$) materials are shown in Figure 5A–F.

3.3. Effects of α -NAA Orientation on the Photoluminescent Properties of α -NAA–HES/LDH ($x\%$). **3.3.1. UV–vis Absorption Spectra and Fluorescence Emission Spectra of α -NAA in Solution and in the LDH Matrix.** The UV–vis absorption spectra of α -NAA in solution and α -NAA–HES/

LDH ($x\%$) samples were measured and displayed in Figure 6. The UV–vis absorption band of α -NAA–HES/LDH ($x\%$) (curves b, c, d, e, f, and g) becomes broader than that of the α -NAA solution sample (curve a), which is the result of homogeneous broadening due to the existence of a continuous set of vibrational sublevels in each electronic state.¹⁷ On the other hand, the maximum absorption peak shifts to longer wavelengths compared with the pristine α -NAA sample. The layer of LDH provides a more rigid and constrained environment for α -NAA, resulting in an intramolecular charge-transfer character to the π – π transition.¹⁸ It can be also found that a progressive red-shift of the absorption band with increasingly stronger intensity was observed (from 287 to 294 nm) upon the increase of α -NAA content. The shift is related to the α -NAA intermolecular interactions, especially π – π interaction,¹⁹ resulting from the more ordered and dense packing of α -NAA molecules.

To further clarify the effects of the α -NAA orientation in the LDH matrix on the photophysical properties, the fluorescence emission spectra of α -NAA–HES/LDH ($x\%$) were recorded (shown in Figure 7). Notably, the maximum emission peak of α -NAA–HES/LDH ($x\%$) (337–340 nm, curves a–g in Figure 7) shifts to a shorter wavelength with respect to the pure α -NAA solid powder (345 nm, Figure 7h) with enhanced fluorescence intensity. These can mainly be ascribed to the host–guest and guest–guest interactions. Martínez and co-workers¹⁵ have demonstrated that a more rigid and constrained environment reduces the internal conversion processes and improves fluorescence intensity of guest molecule. Moreover, the emission peak shows a small red-shift (from 337 to 340 nm) upon increasing the loading of the α -NAA (from 12.1% to 100%). It can be seen from the inset of Figure 7 that the fluorescence intensity increases at first to a maximum and then decreases as the increase of the ratio of α -NAA to HES. The optimal luminous intensity presents in the sample of 15.1%. This behavior can be attributed to the change in the state of the interlayer α -NAA molecule. The dye exhibits single molecular luminescence with low α -NAA concentrations, accounting for the increase in the luminous intensity first, and the J- or H-type dye aggregation forms when the content of α -NAA increases to a certain concentration, resulting in the red-shift of emission spectra and the fluorescence quenching. The tunable fluorescence

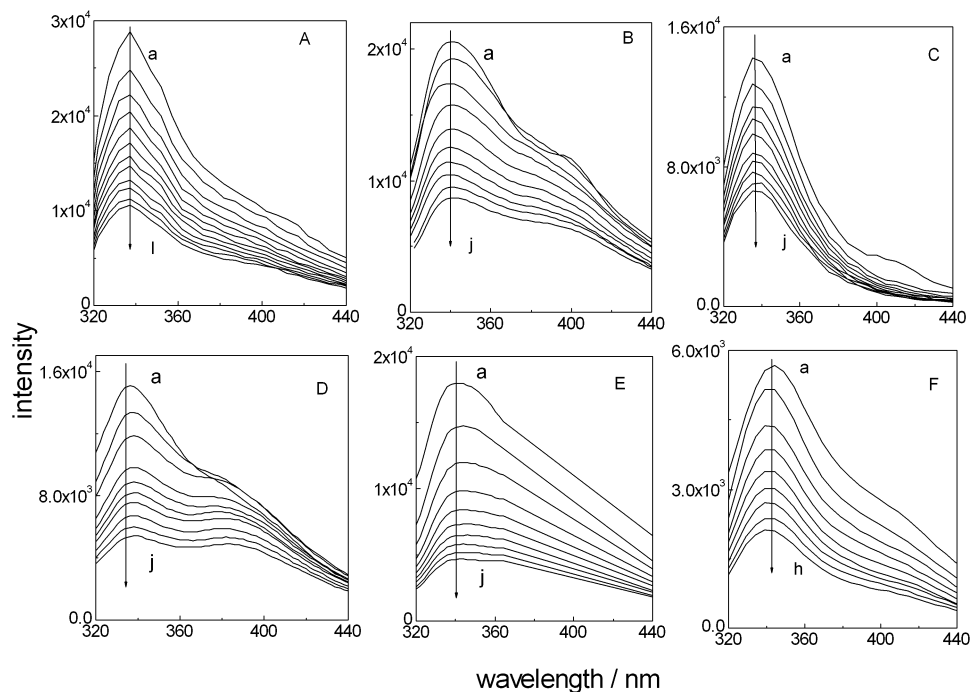


Figure 9. TRES for the sample of α -NAA–HES/LDH ($x\%$): (A) $x = 12.1\%$, (B) $x = 15.1\%$, (C) $x = 20.0\%$, (D) $x = 23.3\%$, (E) $x = 30.0\%$, and (F) $x = 34.4\%$; spectra were recorded after excitation at every 3 ns interval.

maximum is an important factor to be considered in the development of new optical materials in the solid state. The results above indicate that the photophysical properties of guest molecules depend not only on the effect of the matrix (i.e., rigid and confined environment, host–guest interactions, etc.) but also on the distribution and orientation of the chromophore in the LDH matrix (guest–guest interactions).

3.3.2. Fluorescence Lifetime of α -NAA. α -NAA in solution and in the LDH matrix with various contents were studied by detecting their fluorescence decays, with excitation and emission wavelengths of 280 and 337 nm, respectively. The fluorescence lifetimes were obtained by fitting the decay profiles with one-exponential and double-exponential forms, respectively, and the results were shown in Figure S5 and Table 2. The multiexponential decay curves were usually observed in solid samples and can be attributed to highly heterogeneous environments for the molecules in the solid surfaces.²⁰ A similar conclusion has been reported by other researchers in the study of intercalation of Rhodamine 6G (R6G) into Laponite clay.¹⁵ However, it can be found in this work that the r^2 and χ^2/dof (dof: degrees of freedom) of all of the fluorescence decay curves fitted by the one-exponential function are better than those of the double-exponential form. Figure 8 displays the fluorescence lifetime of α -NAA–HES/LDH ($x\%$) as a function of $x\%$. This one-exponential behavior may be related to the reason that the intercalated α -NAA molecular anion does not reorient or preferentially orient with respect to the polarized excitation light, confirming that only one species of α -NAA exists in the LDH matrix for each sample. As shown in Table 2 and Figure 8, the fluorescence lifetime of α -NAA–HES/LDH ($x\%$) increases significantly as x increases from 12.1% to 20.0%, while it turns to decrease with a further increase of $x\%$, because of the formation of aggregation as indicated by the results of fluorescence and absorption spectra. As a result, the longest fluorescence lifetime obtained by one-exponential fitting is presented for the sample of α -NAA–HES/LDH (20.0%).

Furthermore, it was found from Figure 8 that the fluorescence lifetime of α -NAA–HES/LDH ($x\%$) is much longer than that

of α -NAA in aqueous solution (28.5 ns) when x is lower than 23.3%, while it becomes shorter than in solution as x is above 30.0%. The long lifetime ($x\% \leq 23.3\%$) possibly originates from the decrease in internal mobility, flexibility, and the internal conversion processes of α -NAA due to the hydrogen bonding and electrostatic interaction between α -NAA and LDH layers. Meanwhile, the introduction of the HES surfactant in the galleries of LDH enhances the emission efficiency of α -NAA to some extent. Ogawa and Kuroda²¹ reported that surfactants or organic solvents can alter the aggregation of photoactive species. In our opinion, the intercalated long-chain surfactant achieved a nonpolar interlayer environment, which homogeneously diluted and effectively isolated the interlayer α -NAA molecular anions. The shorter lifetime than that of the α -NAA solution ($x\% \geq 30.0\%$) roots in the formation of aggregates as indicated by the results of fluorescence and absorption spectra.

3.3.3. TRES of α -NAA–HES/LDH ($x\%$). Time-resolved emission spectroscopy is also a valid method to obtain the information on the structure of α -NAA molecular anion in the α -NAA–HES/LDH matrix. Figure 9A–F ($x = 12.1\%$, 15.1%, 20.0%, 23.3%, 30.0%, and 34.4%, respectively) shows that the maximum emission peak does not change during their fluorescence lifetime. The absence of time-dependent fluorescence anisotropy reveals that the α -NAA molecule does not reorient or readsorb in the time scale of the fluorescence lifetime. In addition, the results rule out the presence of different α -NAA species with different emission energies for a specific sample, in agreement with the independence of the analysis wavelength on $(D_{\text{HV}})^{\text{cor}}$ (Figure 4). Thus, the time-resolved measurements further confirm the results obtained by UV–vis absorption, steady-state fluorescence spectra, and fluorescence lifetime measurement that the α -NAA is accommodated in the inorganic matrix mainly as the monomer form with $x \leq 23.3\%$, while the J-aggregate comes into formation when $x \geq 30.0\%$.

4. Conclusion

The α -NAA and HES were co-intercalated between sheets of Zn_2Al LDH by the anion exchange method, and thin films

of α -NAA–HES/LDH ($x = 12.1\%$, 15.1% , 20.0% , 23.3% , 30.0% , and 34.4%) with a well c -orientation verified by XRD and SEM were obtained by the solvent evaporation method on Si substrates. On the basis of the results from XRD and fluorescence polarization, the orientation Ψ angles of the α -NAA molecule in the LDH matrix were calculated to be 59° ($x = 12.1\%$), 61° ($x = 15.1\%$), 64° ($x = 20.0\%$), 65° ($x = 23.3\%$), 68° ($x = 30.0\%$), and 71° ($x = 34.4\%$), respectively. Furthermore, the fluorescence wavelength, emission intensity, and lifetime correlate with the orientation of α -NAA remarkably and can be finely controlled by varying the fluorophore content in a rigid and constrained environment of the host. The optimal luminous intensity and the longest fluorescence lifetime of α -NAA–HES/LDH ($x\%$) can be obtained with an x value ranging from 15 to 20%. Therefore, this work presents a successful paradigm for accurately modulating photoluminescent properties of chromophore–LDH materials by simply changing the relative loading of the chromophore and coexisting anion in the LDH matrix. The controllability of the aggregate state of the fluorophore as well as its photoluminescent properties (wavelength, emission intensity, and lifetime) based upon the restrained geometry of the host and the guest–guest interaction creates new opportunities for the design and application of these intercalation compounds in the field of photoluminescent materials, nonlinear optics, and polarized luminescent materials.

Acknowledgment. This project was supported by the National Natural Science Foundation of China, the 111 Project (Grant No.: B07004), the 973 Program (Grant No.: 2009CB939802), and the Program for Changjiang Scholars and Innovative Research Team in University (Grant No.: IRT0406).

Supporting Information Available: Three-dimensional perspective for the experimental setup (Figure S1). The fwhm of XRD patterns (Figure S2). The linear relationship between d_{003} of α -NAA–HES/LDH ($x\%$) and x (Figure S3). FT-IR spectra (Figure S4). Fluorescence decay curves and residual plots of fits (Figure S5). This material is available free of charge via the Internet at <http://pubs.acs.org>.

References and Notes

- (1) (a) Seebacher, C.; Rau, J.; Deeg, F. W.; Brauchle, C.; Altmaier, S.; Jäger, R.; Behrens, P. *Adv. Mater.* **2001**, *13*, 1374. (b) Schulz, G. E.; Wöhrle, D.; Duffel, B. V.; Schoonheydt, R. A. *Microporous Mesoporous Mater.* **2002**, *51*, 91. (c) Ganschow, M.; Wark, M.; Wöhrle, D.; Schulz, E. G. *Angew. Chem., Int. Ed.* **2000**, *112*, 167. (d) Ganschow, M.; Wark, M.; Wöhrle, D.; Schulz, E. G. *Angew. Chem., Int. Ed.* **2000**, *39*, 160. (e) Reck, G.; Marlow, F.; Kornatowski, J.; Hill, W.; Caro, J. *J. Phys. Chem.* **1996**, *100*, 1698. (f) Marlow, F.; Goor, G.; Behrens, P. *Adv. Mater.* **1999**, *11*, 238.
- (2) (a) Umemura, Y.; Yamagishi, A.; Schoonheydt, R. A.; Persons, A.; De Schryver, F. *J. Am. Chem. Soc.* **2002**, *124*, 992. (b) Lee, H. C.; Lee, T. W.; Lim, Y. T.; Park, O. O. *Appl. Clay Sci.* **2002**, *21*, 287.
- (3) Leroux, F.; Taviot, C. G. *J. Mater. Chem.* **2005**, *15*, 3628.
- (4) Pesie, L.; Salipurovie, S.; Markovie, V.; Vucelie, D.; Kagunya, W.; Johns, W. *J. Mater. Chem.* **1992**, *2*, 1069.
- (5) Latterini, L.; Nocchetti, M.; Aloisi, G. G.; Costantino, U.; Elisei, F. *Inorg. Chim. Acta* **2007**, *360*, 728.
- (6) (a) Bauer, J.; Behrens, P.; Speckbacher, M.; Langhals, H. *Adv. Funct. Mater.* **2003**, *13*, 241. (b) Ukrainczyk, L.; Chibwe, M.; Pinnavaia, T. J.; Boyd, S. A. *J. Phys. Chem.* **1994**, *98*, 2668. (c) Saito, T.; Kadokawa, J. I.; Tagaya, H. *Trans. Mater. Res. Soc. Jpn.* **2001**, *26*, 503. (d) Hwang, S. H.; Han, Y. S.; Choy, J. H. *Bull. Korean Chem. Soc.* **2001**, *22*, 1019. (e) Cooper, S.; Dutta, P. K. *J. Phys. Chem.* **1990**, *94*, 114.
- (7) Costantino, U.; Coletti, N.; Nocchetti, M.; Aloisi, G. G.; Elisei, F. *Langmuir* **1999**, *15*, 4454.
- (8) Shi, W. Y.; Wei, M.; Lu, J.; Li, F.; He, J.; David, G. E.; Duan, X. *J. Phys. Chem. C* **2008**, *112*, 19886.
- (9) (a) Aloisi, G. G.; Costantino, U.; Elisei, F.; Latterini, L.; Natali, C.; Nocchetti, M. *J. Mater. Chem.* **2002**, *12*, 3316. (b) Newman, S. P.; Cristina, T. D.; Coveney, P. V.; Jones, W. *Langmuir* **2002**, *18*, 2933. (c) Newman, S. P.; Samuel, J. W.; Coveney, P. V.; Jones, W. *J. Phys. Chem. B* **1998**, *102*, 6710.
- (10) Bontchev, P. P.; Liu, S.; Krumhansl, J. L.; Voigt, J. *Chem. Mater.* **2003**, *15*, 3669.
- (11) (a) Hagerman, M. E.; Salamone, S. J.; Herbst, R. W.; Payeur, A. L. *Chem. Mater.* **2003**, *15*, 443. (b) Bújdak, J.; Iyi, N.; Fujita, T. *J. Colloid Interface Sci.* **2003**, *262*, 282. (c) Miyamoto, N.; Kawai, R.; Kuroda, K.; Ogawa, M. *Appl. Clay Sci.* **2001**, *19*, 39.
- (12) Valeur, B. *Molecular Fluorescence: Principles and Applications*; Wiley-VCH: Weinheim, Germany, 2002; p 27.
- (13) Valeur, B. *Molecular Fluorescence: Principles and Applications*; Wiley-VCH: Weinheim, Germany, 2002; p 37.
- (14) (a) Slyadneva, O. N.; Slyadnev, M. N.; Tsukanova, V. M.; Inoue, T.; Harata, A.; Ogawa, T. *Langmuir* **1999**, *15*, 8651. (b) López, A. F.; Martínez, M. V. *J. Photochem. Photobiol., A* **2006**, *181*, 44. (c) López, A. F.; Martínez, M. V. *Chem. Mater.* **2006**, *18*, 1407.
- (15) (a) Michl, J.; Thulstrup, E. W. *Spectroscopy with Polarized Light*; VCH Publishers: New York, 1986. (b) Kliger, D. S.; Lewis, J. W.; Randall, C. E. *Polarized Light in Optics and Spectroscopy*; Academic Press, Inc.: London, 1990. (c) Lakowicz, J. R. *Principles of Fluorescence Spectroscopy*, 2nd ed.; Kluwer Academic: New York, 1999. (d) Valeur, B. *Molecular Fluorescence: Principles and Applications*; Wiley-VCH: Weinheim, Germany, 2002. (e) Martínez, M. V.; López, A. F.; Banúelos, P. J.; López, A. I. *J. Phys. Chem. B* **2005**, *109*, 7443.
- (16) (a) Wu, J. J.; Gross, A. F.; Tolbert, S. H. *J. Phys. Chem. B* **1999**, *103*, 2374. (b) Tan, C. Y.; Evrim, A.; Müller, J. G.; Mauricio, R. P.; Kleiman, V. D.; Schanze, K. S. *J. Am. Chem. Soc.* **2004**, *126*, 13685. (c) Valeur, B. *Molecular Fluorescence: Principles and Applications*; Wiley-VCH: Weinheim, Germany, 2002; Chapters 5 and 6.
- (17) Nemkovich, N. A.; Rubinov, A. N.; Tomin, I. T. In *Inhomogeneous Broadening of Electronic Spectra of Dye Molecules in Solutions*; Lakowicz, J. R., Ed.; Topics in Fluorescence Spectroscopy, Vol. 2; Springer: New York, 1991; p 367.
- (18) Valeur, B. *Molecular Fluorescence: Principles and Applications*; Wiley-VCH: Weinheim, Germany, 2002; p 58.
- (19) Costantino, U.; Coletti, N.; Nocchetti, M.; Aloisi, G. G.; Elisei, F.; Latterini, L. *Langmuir* **2000**, *16*, 10351.
- (20) (a) Rurack, K.; Hoffman, K.; Al-Soufi, W.; Resch-Genger, U. *J. Phys. Chem. B* **2002**, *106*, 9744. (b) Wiederrecht, G. P.; Sandi, G.; Carrado, K. A.; Seifert, S. *Chem. Mater.* **2001**, *13*, 4233. (c) Latterini, L.; Nocchetti, M.; Aloisi, G. G.; Costantino, U.; Schryver, F. C. D.; Elisei, F. *Langmuir* **2007**, *23*, 12337.
- (21) Ogawa, M.; Kuroda, K. *Chem. Rev.* **1995**, *95*, 399.